Electrostatics of a Simple Membrane Model Using Green's Functions Formalism

Eberhard von Kitzing* and Dikeos Mario Soumpasis#
*Abteilung Zellphysiologie, Max-Planck-Institut für medizinische Forschung, D-69028 Heidelberg, and #Biocomputation Group, Max-Planck-Institut für biophysikalische Chemie, D-37077 Göttingen, Germany

ABSTRACT The electrostatics of a simple membrane model picturing a lipid bilayer as a low dielectric constant slab immersed in a homogeneous medium of high dielectric constant (water) can be accurately computed using the exact Green's functions obtainable for this geometry. We present an extensive discussion of the analysis and numerical aspects of the problem and apply the formalism and algorithms developed to the computation of the energy profiles of a test charge (e.g., ion) across the bilayer and a molecular model of the acetylcholine receptor channel embedded in it. The Green's function approach is a very convenient tool for the computer simulation of ionic transport across membrane channels and other membrane problems where a good and computationally efficient first-order treatment of dielectric polarization effects is crucial.

INTRODUCTION

The theoretical modeling of ion transport across membranes is a topic of continuous interest in computational biophysics (Andersen and Koeppe, 1992; Bek and Jakobsson, 1994; Cooper et al., 1985; Eisenberg, 1996a,b; Jakobsson, 1993; Jordan, 1993; Partenskii et al., 1994; Syganow and von Kitzing, 1995). Any quantitative treatment of this problem involves 1) specification of a structural model for the membrane and the protein channel of interest, 2) determination of the interactions present in this system, and 3) computation of the dynamic quantities (e.g., the ion currents) based on 1) and 2) in connection with a theoretical model for the motions.

Thanks to the availability of powerful computers, microscopic simulation techniques such as molecular dynamics and Brownian dynamics have progressively replaced the more macroscopic treatments of the dynamics via the Nernst-Planck and/or the Eyring absolute rate theories. Thus, more detailed structural models can now be studied (Alvarez et al., 1992; Åqist and Warshel, 1989; Cafiso, 1994; Jakobsson, 1993; Jakobsson and Chiu, 1988; Jordan, 1990; Kerr et al., 1994; Oiki et al., 1990; Partenskii and Jordan, 1992b; Polymeropoulos and Brickmann, 1985; Roux and Karplus, 1994; Sansom, 1993; Veresov, 1994). The adequate description of the electrostatic interactions present in the system membrane-channel water ions, however, remains a problem. The appropriate calculation of electrostatic interaction in biomolecules is still a subject of considerable research (Bharadwaj et al., 1995; Darden et al., 1993; Harvey, 1989; Kuwajima and Warshel, 1988; Lee and Warshel, 1992; Luty and van Gunsteren, 1996; Schaefer and Karplus, 1996; Schreiber and Steinhauser, 1992; Sharp, 1991; Sklenar et al., 1990; van Gunsteren and Berendsen, 1990). Because of its great computational complexity, it cannot be adequately handled by computer simulation techniques alone. The so-called image or dielectric polarization effects are a typical example of this situation. If it were possible to model every molecule in the system (i.e., lipids, protein, ions, water) microscopically, i.e., on a quantum mechanical level, the bare Coulomb law with a dielectric constant of 1 would suffice to describe the electrostatics completely. Clearly, such a structural description of the system is not possible, either now or in the near future. Therefore, large parts of the system (e.g., the membrane and the solvent surrounding it) have to be modeled more approximately (e.g., as dielectric continua). This immediately gives rise to very complicated effective electrostatic interactions due to the coupling of the charges to the dielectric polarization fields caused by the dielectric boundaries (e.g., membrane-water).

The determination of electrostatic fields and interactions in such a heterogeneous dielectric is of course a classical boundary value problem in electrostatics (Jackson, 1962; Smythe, 1939). Analytical results are restricted to particular geometries of the dielectric boundary surfaces for which the Laplacean can be separated, such as a planar (Jackson, 1962; Smythe, 1939) or a spherical (Kirkwood, 1934) boundary.

To circumvent these problems, many heuristic approaches have been introduced to account for such effects by means of ad hoc formulas. In the case of very small molecules, the aqueous environment may be represented by using a spherical cavity. Electric monopole, dipole, and higher moments may be used to approximate the effect of the solvent (Dosen-Micovic and Allinger, 1978). Recently, solvation effects were simulated by using the solvent-accessible surface approach in molecular mechanics (Eisenberg et al., 1989; Holm and Sander, 1992; Schiffer et al., 1993) and semiempirical self-consistent field methods (Cramer

Received for publication 1 May 1995 and in final form 9 May 1996.

Address reprint requests to Dr. Eberhard von Kitzing, Abteilung Zellphysiologie, Max-Planck-Institut für medizinische Forschung, Postfach 10 38 20, D-69028 Heidelberg, Germany. Tel.: 49-6221-486-467; Fax: 49-6221-486-459; E-mail:vkitzing@sunny.mpimf-heidelberg.mpg.de.

0006-3495/96/08/795/16 $2.00

and Truhlar, 1992). These methods may make it possible to obtain some fairly good estimates of the solvation free energy; however, such approaches certainly cannot account for the influence of the solvent on the solute electrostatic field.

For this reason, current studies, especially in the field of protein biophysics, resort to entirely numerical solutions of either the Poisson equation (Mohan et al., 1992; Sharp, 1991; Zacharias et al., 1994) or, equivalently, the integral equation for the polarization surface charge density (Jordan, 1982, 1983; Juffer and Berendsen, 1993; Juffer et al., 1991; Levitt, 1978a,b, 1991; Vorobjev et al., 1992; Zauhar and Morgan, 1985, 1988; Zhexin et al., 1994). The advantage of these techniques is that practically any dielectric boundary shape can be handled. Their computational cost, however, is very large and their usefulness for dynamic studies, e.g., of ion transport across membranes of protein motions, is extremely limited. Essentially for every charge configuration created by the dynamics, one must numerically solve three-dimensional partial differential or integral equations to compute the forces leading to the next configuration. To circumvent this problem, approximate approaches to solving these difficulties are proposed (Schaefer and Karplus, 1996; Sklenar et al., 1990; Still et al., 1990; Stouten et al., 1993).

In view of these facts, it is more fruitful to reanalyze the problem in an effort to reduce the computational complexity to manageable size. Such theoretical work has been initiated (Shaw, 1985; Tlewelling and Hubbel, 1986), and more is needed. The present paper is concerned with the efficient computation of the effective electrostatic interactions in a very simple membrane-water dielectric continuum model, which, however, serves as the structural background for more detailed models of ion channels embedded in it.

THEORY

For the purpose of computing the electrostatics, including the relevant image effects to all orders, the model depicted in Fig. 1 is considered. A laterally infinite slab of thickness d and dielectric constant ϵ_M (the membrane) separates the space into three regions: 1 and 3 being occupied by the solvent modeled by a dielectric constant of ϵ_W. Point charges Q_ν, $\nu \in \{1, \ldots, M\}$ at positions $\mathbf{r}'_\nu$ in regions 2 model charged groups of a structural model of the channel, and charges q_k, $k \in \{1, \ldots, N\}$ at positions $\mathbf{r}_k$ model the ions present in the system or also possibly the partial charges of another charged molecule.

In some of the previous work on the electrostatic problem of ionic transport (Jordan, 1981, 1982, 1983, 1993; Levitt, 1978a,b; Parsegian, 1969, 1975; Partenskii and Jordan, 1992b), slightly different dielectric models have been studied, using a cylindrical pore in the slab to represent the channel (see Jordan, 1993; Partenskii and Jordan, 1992b, for a recent review). This kind of geometry assumes that local ion-water and ion-channel wall interactions can be accounted for by means of a continuum model. As shown previously (Dorman et al., 1996; Roux, 1993; Sancho et al., 1995), the local interaction of the ion with water and the atoms of the channel wall contributes considerably to the energy profile and consequently to the ionic permeability. To model these properties of the ion channel by means of continuum approximations would certainly require more complex forms of the dielectric constant as the simple linear one. Nonlocal effects would have to be included (Kornyshev and Sutmann, 1996; Partenskii and Jordan, 1992a). Consequently, adding a cylinder to the membrane with a dielectric constant different from that of the channel protein complicates the mathematics without adding anything significantly new to the physics of the problem (i.e., the qualitative form of the self energy and the ion-ion interaction modified by the presence of the low dielectric membrane does not change).

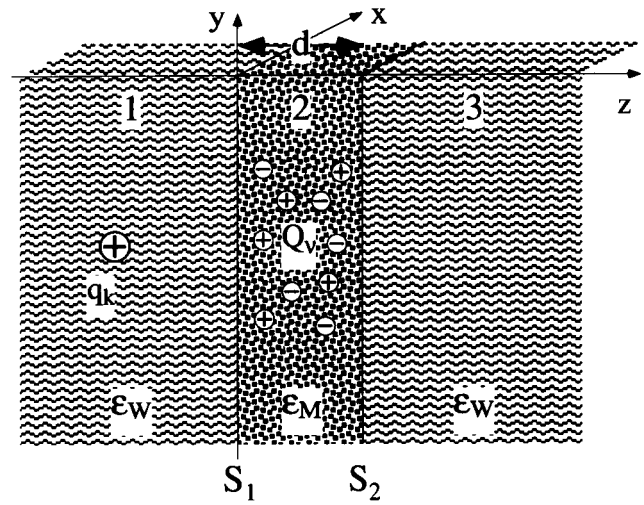

FIGURE 1 The dielectric properties of a membrane in water consisting of a lipid bilayer containing membrane proteins are modeled by a laterally infinite slab with a thickness d and a dielectric constant of ϵ_M. This slab separates the space into three regions: 1 and 3 represent the water phase with a dielectric constant of $\epsilon_W \approx 80$, and region 2 represents the membrane. The surfaces S_1 and S_2 separate the regions 1/2 and 2/3, respectively. The membrane may contain several fixed charges Q_ν representing the partial charges of lipid molecule or membrane protein atoms. The interaction of test charges q_k with the membrane dielectric properties and the membrane charges Q_ν is considered in this study.

Within the continuum approach the protein material comprising such a channel is dielectrically indistinguishable from the surrounding lipid environment; they have very similar dielectric constants (Dilger et al., 1982; Simonson et al., 1991; Tredgold and Hole, 1976; Warshel, 1987), on the order of $2 < \epsilon_M < 6$. Even if the detailed structural channel model includes water molecules at least inside the pore of the channel, they certainly do not constitute a liquid water phase of $\epsilon_W \approx 80$, because of interactions with the protein and their small number (Partenskii et al., 1991; Partenskii and Jordan, 1992a).

It is therefore legitimate to focus on the predominant polarization effects due to the large dielectric discontinuity between the membrane and the water phases and to use the simple model depicted in Fig. 1. It includes the long-range

part of the interaction, i.e., the interaction of the ions with the dipoles of distant water molecules. This particular part of the problem is difficult to evaluate by explicit approaches. For fairly realistic simulation of ion transport, the local environment, consisting of water molecules and the atoms of the walls of the channel pore, should be included explicitly.

Green function description of the electrostatics

A convenient method of calculating the electrostatic potential in the presence of charges and boundary conditions is to introduce the Green's function of the problem (Jackson, 1962). Knowledge of the Green's functions $\mathcal{G}_i(\mathbf{r}, \mathbf{r}')$, $i \in \{1, 2, 3\}$ is essential for a complete description of the electrostatics. $\mathcal{G}_2(\mathbf{r}, \mathbf{r}')$ is the electric potential created by a unit positive point charge located at $\mathbf{r}'$ in region 2 (the source point) at a point $\mathbf{r}$ (the field point), which can be anywhere. It satisfies the Poisson equation for a point charge:

$$\nabla^2 \mathcal{G}_2(\mathbf{r}, \mathbf{r}') = -4\pi\delta(\mathbf{r} - \mathbf{r}'), \tag{1}$$

where δ is the Dirac delta function and ∇^2 is the Laplacean. The following boundary conditions must be fulfilled at the interface S_1 (see Fig. 1):

$$\lim_{z\to 0_+} \mathcal{G}_2(\mathbf{r}, \mathbf{r}') = \lim_{z\to 0_-} \mathcal{G}_2(\mathbf{r}, \mathbf{r}') \tag{1a}$$

$$\lim_{z\to 0_+} \epsilon_W \frac{\partial}{\partial z} \mathcal{G}_2(\mathbf{r}, \mathbf{r}') = \lim_{z\to 0_-} \epsilon_M \frac{\partial}{\partial z} \mathcal{G}_2(\mathbf{r}, \mathbf{r}'), \tag{1b}$$

where $\mathbf{r} = (x, y, z)$ and $z \to 0_+$ ($z \to 0_-$) means that the limit is taken from the right-hand side (from the left-hand side) of the interface S_1. Similar boundary conditions apply to interface S_2 ($z \to d_\pm$) as well. The other two Green's functions $\mathcal{G}_1(\mathbf{r}, \mathbf{r}')$ and $\mathcal{G}_3(\mathbf{r}, \mathbf{r}')$ are defined in an exactly analogous manner, with the source point $\mathbf{r}'$ being in region 1 and 3, respectively. Here only point charges are considered, and not smeared-out surface charge densities.

Next, we represent the Green's functions (e.g., $\mathcal{G}_2$) in a form that is more convenient for the subsequent discussion and computations, namely;

$$\begin{aligned}\mathcal{G}_2(\mathbf{r}, \mathbf{r}') = {} & \frac{1}{\epsilon_M \|\mathbf{r} - \mathbf{r}'\|} \\ & + \int\int_{-\infty}^{+\infty} \frac{\sigma_1(\mathbf{u}|\mathbf{r}')\, du_1\, du_2}{[(x-u_1)^2 + (y-u_2)^2 + z^2]^{1/2}} \\ & + \int\int_{-\infty}^{+\infty} \frac{\sigma_2(\mathbf{u}|\mathbf{r}')\, du_1\, du_2}{[(x-u_1)^2 + (y-u_2)^2 + (z-d)^2]^{1/2}}.\end{aligned} \tag{2}$$

The first right-hand-side Coulomb term is the Green's function in the absence of any dielectric inhomogeneity, whereas the second and third terms are the polarization potentials at $\mathbf{r}$ arising from the (yet unknown) surface polarization charge densities $\sigma_1(\mathbf{u}|\mathbf{r}')$ and $\sigma_2(\mathbf{u}|\mathbf{r}')$ induced on the dielectric boundary surfaces S_1 and S_2, respectively, due to the presence of the source charge at $\mathbf{r}'$. The vector $\mathbf{u} = (u_1, u_2)$ is the x and y components of a point on the surface S_1 or S_2 (see Fig. 1).

Using the representation of Eq. 2, it is now possible to reduce the solution of the boundary value problem (eqs. 1, 1a, and 1b) to that of finding $\sigma_1(\mathbf{u}|\mathbf{r}')$ and $\sigma_2(\mathbf{u}|\mathbf{r}')$. In the case of our planar slab geometry, this can be done following procedures described by others (Mahanty and Ninham, 1976; Stakold, 1968).

The boundary condition 1a (continuity of the potential) is automatically satisfied by the $\mathcal{G}_2$ of Eq. 2. Applying the boundary condition 1b to Eq. 2 and using the identity

$$\begin{aligned}\lim_{z\to 0_\pm} \frac{z}{[(x-u_1)^2 + (y-u_2)^2 + z^2]^{3/2}} = {} & \\ & \pm 2\pi\delta(x-u_1)\cdot\delta(y-u_2)\end{aligned} \tag{3}$$

at the interface $z = 0$ and a similar one at $z = d$ yields a system of two coupled linear integral equations for $\sigma(\mathbf{u}|\mathbf{v}')$ and $\sigma(\mathbf{u}|\mathbf{v}')$:

$$\begin{aligned}& + 2\pi(\epsilon_W + \epsilon_M)\sigma_1(\mathbf{u}|\mathbf{r}') \\ & \quad + (\epsilon_W - \epsilon_M)d \int\int_{-\infty}^{+\infty} \frac{\sigma_2(\mathbf{v}|\mathbf{r}')\, dv_1\, dv_2}{[(u_1-v_1)^2 + (u_2-v_2)^2 + d^2]^{3/2}} \\ & \quad = -\frac{(\epsilon_W - \epsilon_M)z'}{[(x'-u_1)^2 + (y'-u_2)^2 + z'^2]^{3/2}} \\ & -2\pi(\epsilon_W + \epsilon_M)\sigma_2(\mathbf{u}|\mathbf{r}') \\ & \quad - (\epsilon_W - \epsilon_M)d \int\int_{-\infty}^{+\infty} \frac{\sigma_1(\mathbf{v}|\mathbf{r}')\, dv_1\, dv_2}{[(u_1-v_1)^2 + (u_2-v_2)^2 + d^2]^{3/2}} \\ & \quad = +\frac{(\epsilon_W - \epsilon_M)(d-z')}{[(x'-u_1)^2 + (y'-u_2)^2 + (d-z')^2]^{3/2}},\end{aligned} \tag{4}$$

which can be solved using two-dimensional Fourier transformations. Using these solutions and cylindrical coordinates in κ space one obtains after some algebra:

$$\begin{aligned}\mathcal{G}_2(\mathbf{r}, \mathbf{r}') = {} & \frac{1}{\epsilon_M \|\mathbf{r} - \mathbf{r}'\|} + \frac{1}{\epsilon_M} \int_0^\infty \frac{J_0(\kappa\|\mathbf{R} - \mathbf{R}'\|)}{1 - \Delta^2 \exp(-2\kappa d)} \\ & \{-\Delta \exp[-\kappa(|z| + |z'|)] \\ & \quad + \Delta^2 \exp[-\kappa(|d-z| + |z'| + d)] \\ & \quad - \Delta \exp[-\kappa(|d-z| + |d-z'|)] \\ & \quad + \Delta^2 \exp[-\kappa(|z| + |d-z'| + d)]\}\, d\kappa,\end{aligned} \tag{5}$$

where J_0 is the zeroth-order Bessel function, $\mathbf{R} = (x, y)$, $\mathbf{R}' = (x', y')$, and $\Delta = (\epsilon_W - \epsilon_M)/(\epsilon_W + \epsilon_M)$.

The other two Green's functions for regions 1 and 3 are

obtained in a similar manner:

$$\mathcal{G}_1(\mathbf{r}, \mathbf{r}') = \frac{1}{\epsilon_W \|\mathbf{r} - \mathbf{r}'\|} + \frac{1}{\epsilon_W} \int_0^\infty \frac{J_0(\kappa \|\mathbf{R} - \mathbf{R}'\|)}{1 - \Delta^2 \exp(-2\kappa d)}$$
$$\{ + \Delta \exp[-\kappa(|z| + |z'|)]$$
$$- \Delta^2 \exp[-\kappa(|d - z| + |z'| + d)]$$
$$- \Delta \exp[-\kappa(|d - z| + |d - z'|)]$$
$$+ \Delta^2 \exp[-\kappa(|z| + |d - z'| + d)]\} \, d\kappa \quad (6)$$

$$\mathcal{G}_3(\mathbf{r}, \mathbf{r}') = \frac{1}{\epsilon_W \|\mathbf{r} - \mathbf{r}'\|} + \frac{1}{\epsilon_W} \int_0^\infty \frac{J_0(\kappa \|\mathbf{R} - \mathbf{R}'\|)}{1 - \Delta^2 \exp(-2\kappa d)}$$
$$\{ - \Delta \exp[-\kappa(|z| + |z'|)]$$
$$+ \Delta^2 \exp[-\kappa(|d - z| + |z'| + d)]$$
$$+ \Delta \exp[-\kappa(|d - z| + |d - z'|)]$$
$$- \Delta^2 \exp[-\kappa(|z| + |d - z'| + d)]\} \, d\kappa. \quad (7)$$

Using these three Green's functions, one is in a position to compute all relevant electrostatic interactions and properties of systems of point charges residing anywhere in space, for the dielectric model at hand. For instance, to obtain the self-energy $U_{2S}(\mathbf{r})$ of a point ion of charge q at $\mathbf{r}$ in region 2 (the membrane) one sets $z = z'$, $\mathbf{R} = \mathbf{R}'$ in the second right-hand-side term of Eq. 5 (the polarization term) and obtains

$$U_{2S}(\mathbf{r}) = \frac{1}{2} \frac{q^2}{\epsilon_M} \phi_S(\mathbf{r}) \quad (8)$$
$$= -\frac{1}{2} \frac{q^2}{\epsilon_M} \int_0^\infty \frac{\Delta \exp(-2\kappa z) + \Delta \exp(-2\kappa(d - z)) - 2\Delta^2 \exp(-2\kappa d)}{1 - \Delta^2 \exp(-2\kappa d)} \, d\kappa.$$

Expanding the geometric series in the integrand one obtains:

$$U_{2S}(\mathbf{r}) = -\frac{q^2}{2\epsilon_M d} \times \quad (9)$$
$$\left\{ \frac{1}{2} \sum_{n=0}^{\infty} \left[\frac{\Delta^{2n+1}}{n + z/d} + \frac{\Delta^{2n+1}}{n + 1 - z/d} \right] + \Delta^2 \sum_{n=0}^{\infty} \frac{\Delta^{2n}}{n + 1} \right\},$$

which is identical to Parsegian's expression (Parsegian, 1975) if one shifts the coordinate origin to $d/2$, the origin used there, and sums the last series term.

The present treatment is, of course, much more general compared to that of Parsegian. One can obtain self energy in the other regions using the analogous procedure with Eqs. 6 and 7. In addition, one can also calculate the total energy $U_2(\mathbf{r})$ in the presence of, say, M fixed charges $\{Q_\nu\}$ located at $\{\mathbf{r}_\nu\}$, $\nu \in \{1, \ldots, M\}$ in the membrane via

$$U_2(\mathbf{r}) = \frac{1}{2} \frac{q^2}{\epsilon_M} U_{2S}(\mathbf{r}) + q \sum_{\nu=1}^{M} Q_\nu \mathcal{G}_2(\mathbf{r}, \mathbf{r}_\nu). \quad (10)$$

And finally, the exact electrostatic interaction energies and forces of any number of point charges anywhere in space, including all image effects due to the dielectric discontinuities of the model, can be evaluated by means of this approach. As discussed in the Introduction, this is a necessary prerequisite for accurately modeling the dynamics of ion transport. Technical details concerning the numerical computations are given in the Appendix.

The self energy at the boundaries

The self-potential ϕ_S of a test charge outside or inside the membrane shows a singularity at $z/d = 0$ and $z/d = 1$. This can be seen in Fig. 2 and in the limiting formulas in the Results section (see below):

$$\lim_{z/d \to \pm 0} \phi_S = \mp \frac{\Delta}{2|z|}.$$

This singularity is a consequence of using point charges. The work to bring a point charge from region 1 with dielectric constant ϵ_W into region 2 with ϵ_M is infinite as long as $\epsilon_W \neq \epsilon_M$. However, crystal radii (Hille, 1992) of real ions are different from zero. In many cases the binding of water molecules is rather strong, such that the effective radii r_H of several ionic species should include water molecules (Soumpasis et al., 1987). The energy obtained by transferring a charge from a medium with a dielectric constant ϵ_M into a medium with ϵ_W with a "hydration shell" of

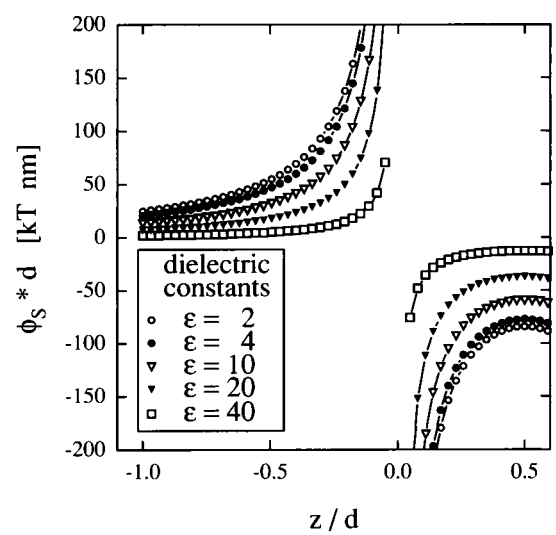

FIGURE 2 The self energy ϕ_S as a function of the position z of a unit charge for membrane dielectric constants ϵ_M between 2 and 40 (see figure legend). The water permittivity ϵ_W is taken to be 80.

radius r_H is given by the well-known Born hydration energy (Born, 1920):

$$E_B = \frac{1}{2}\left(\frac{1}{\epsilon_W} - \frac{1}{\epsilon_M}\right)\frac{q^2}{r_H}. \tag{11}$$

The radius r_H of this hydration shell includes all water molecules that are essentially immobilized by the strong radial electric field of the central ion. This reduces the local molecular polarizability considerably. The water molecules close to the ions will produce an dielectric screening factor close to that of a lipid bilayer or the protein portion of ion channel pores. Parts of the "hydration shell" may be replaced by the side chains of the channel protein when the ion enters the pore. Thus, the effective hydration radius may be larger than the radius of the cross section of the pore (see Fig. 3). The question of the correct values and forms of Born energy is still not solved and is subject to research (Andersen and Koeppe, 1992; Bopp et al., 1996; Born, 1920; Eisenman and Alvarez, 1991; Hawkins et al., 1995; Hummer et al., 1996; Hyun et al., 1995; Kornyshev and Sutmann, 1996; Mohan et al., 1992; Partenskii and Jordan, 1992b; Sharp, 1993; Still et al., 1990; Stokes, 1964, to cite only a few relevant articles).

In this article the hydration radius r_H is taken as a constituent number of the theory, which is varied to study its influence on the self energy of the ions inside the channel, i.e., the height and form of the energy barrier. Physically reasonable values for the hydration radius and consequently Born's energy E_B should be obtained from studies of the energetic requirements to transfer the ion from the water phase into the membrane/channel environment (Åqist and Warshel, 1989a,b; Dorman et al., 1996).

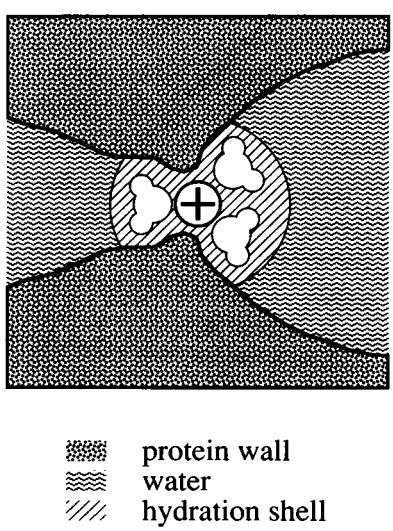

FIGURE 3 The effective dielectric constant of water molecules tightly bound to the ion is close to that of hydrophilic side chains of the channel protein. Thus, the effective radius r_H of the hydration shell around the ion with a low dielectric constant may be larger then the radius of the cross section in the narrowest part of the channel.

If the zero point energy E_0 of the ion in bulk water is defined to be zero, that of the membrane matrix must be $-E_B$:

$$E_0(z) = \begin{cases} -E_B & \text{for } r_H < z < d - r_H \\ 0 & \text{for } z < -r_H \vee d + r_H > z. \end{cases} \tag{12}$$

Now the influence of the hydration shell on the self energy of the ion is studied. Because the dielectric constant inside the hydration shell is chosen to be equal to that of the membrane as long as the ion is completely inside the membrane ($r_H < z < d - r_H$), Born's hydration energy E_B has to be subtracted from the point particle self energy. Two ranges remain to be examined:

$$-r_H < z < r_H \quad \text{and} \quad z \leq -r_H.$$

For $z < -r_H$ the images from the polarization of the hydration shell must be included. Because these effects will vanish faster than the charge-image-charge interaction, this effect is neglected.

For the range $-r_H < z < +r_H$, a spline interpolation is used. From the limiting formulas (see below) at $z \to \pm 0$, the following points on the z axis, z_1 and z_2, are used as the start and end points in the spline interpolation:

$$z_1 = +\frac{\Delta}{E_B}\left[\frac{1}{\epsilon_W} + \frac{1}{[\epsilon_W \epsilon_M]^{1/2}}\right] r_H$$

and

$$z_2 = -\frac{\Delta}{E_B}\left[\frac{1}{\epsilon_M} + \frac{1}{[\epsilon_W \epsilon_M]^{1/2}}\right] r_H.$$

In the limit of $r_H \ll d$ this choice results in a smooth differentiable function for the self energy. For $r_H \simeq d/2$, the z_1 and z_2 values are adjusted accordingly. The situation at the other side of the membrane, at $z = d$, is symmetric and does not require special consideration.

RESULTS AND DISCUSSION

It is the purpose of this article to introduce an exact, nontrivial Green's function for an idealized water-membrane-water system (see Fig. 1) and to apply it to simple situations that help us to understand its major properties. It represents an exact solution for calculating the electrostatic interactions for a distribution of point charges and charge densities in a water-membrane-water system as long as the charges do not pass the water-membrane boundary.

Because of the singularity of the self energy for charges passing the water-membrane boundary, the idea of Born energy E_B was added as a heuristic concept by introducing the hydration radius r_H. The Born energy accounts for the energy required to transfer the ion from the bulk water environment into the membrane/channel environment. This energy difference does depend explicitly on the details of the model of the ion channel, e.g., on how the water inside the channel is modeled. Therefore, the precise value for

Born's energy must be estimated individually for each model. For the purpose of studying the self-energy of an ion in the water-membrane system, Born's energy, i.e., the hydration radius, was introduced merely as a variable number.

By means of the Green's function formalism, the electrostatic energy of a charged atom is determined by the atom's self energy U_S and the mutual electrostatic interaction with all other charged atoms U_ν. Such atoms may be ions or the partially charged atoms of atomic force fields (Aleman et al., 1994; Bayley et al., 1993; Cornell et al., 1995; Dinur and Hagler, 1989; Hagler and Ewig, 1994; Halgren, 1995; Lavery et al., 1984; Pearlman and Kim, 1990; Reynolds et al., 1992). Consequently, this method can be introduced in molecular mechanics and dynamics program packages to simulate the electrostatic properties of membranes and molecules embedded in membranes, e.g., ion channels.

In many practical cases the molecular geometry may deviate considerably from the simple membrane-like form as depicted in Fig. 1. For instance, the acetylcholine receptor channel has a large extracellular funnel (Toyoshima and Unwin, 1988). This situation invites perturbation methods. Shaw (1985) starts from the Green's function of a low-dielectric sphere embedded in a high-dielectric medium. For globular proteins he describes how to account for the deviation from the spherical shape in the electrostatic interactions. The perturbation approach proposed for globular proteins can be reformulated to consider deviations from a membrane-like geometry.

Throughout this article it is assumed that all charges are localized. The screening effect of mobile ions is not included in this approach. Because the counter-ion clouds not only shield the electric field of "real" charges but also their respective images, the effect of the dielectric barrier resulting from the self energy of the ions, i.e., the interaction with their own images, decreases considerably (Boiko, 1993; Syganow and von Kitzing, manuscript in preparation).

The results of the Green's function approach are presented, concentrating on three different aspects. The self energy acts merely as an energy barrier for all charges across the membrane. In some regions, because of the presence of the low-dielectric membrane, the charge-charge interaction may become more strongly screened compared to charge-charge interactions in pure water. As an illustration, the Green's function approach is applied to a molecular model of the pore of the acetylcholine receptor channel.

The self energy

The self energy U_S (see Eqs. 8 and 9) represents the interaction of a test charge with all of its charge images, generated by dielectric inhomogeneities. Fig. 2 shows the point charge self energy as a function of the position of the test charge relative to the membrane.

Because no explicit analytical solution is available, considerations of limiting cases of the charge self energy U_S are useful for understanding its physical implications. The limits involved can be directly obtained from the formulas A3 and A4 given in the Appendix.

If the distance of the charge in solution from the membrane is small compared to the thickness of the membrane d ($-z \ll d$), the case of an "infinitely thick" membrane is obtained (Jackson, 1962):

$$\lim_{z/d \to -0} U_S(z<0) = -\frac{q^2}{\epsilon_W}\frac{\Delta}{2z}. \tag{13}$$

At distances large compared to the membrane thickness d, the interaction of the test charge q with its own mirror images is essentially a monopole-dipole interaction, where the dipole has a dipole-moment of $qd\Delta/(1-\Delta^2)$:

$$\lim_{z/d \to -\infty} U_S(z<0) = \frac{q^2}{\epsilon_W}\frac{\Delta}{1-\Delta^2}\frac{d}{z^2}. \tag{14}$$

Fig. 4 gives the logarithm of the point charge self energy U_S for negative z. The transition between the short-range interactions (slope = -1) and long-range interactions (slope = -2) of the charge with its images is clearly seen. If the difference between the two dielectric constants is small ($\Delta \ll 1$), one has

$$U_S(z<0) \approx -\frac{q^2}{\epsilon_W}\frac{\Delta}{2}\frac{d}{z(d-z)}. \tag{15}$$

The limits of the point charge self energy of a charge inside the membrane agree with those point charge self energies of a charge in solution in the cases of small z (Eq.

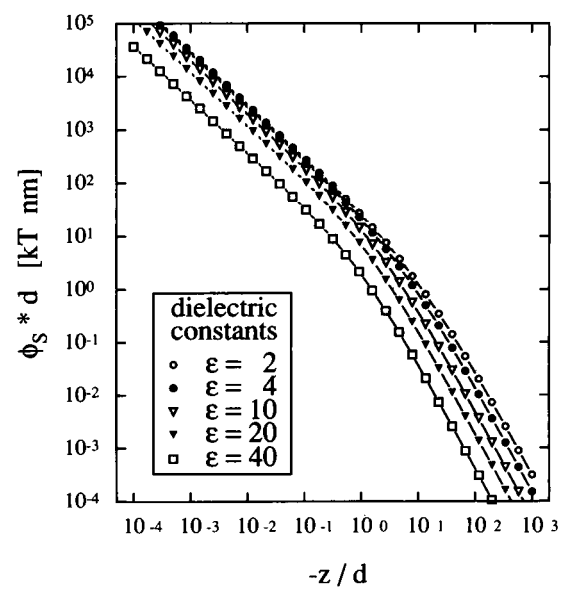

FIGURE 4 A logarithmic plot of the self energy ϕ_S for negative z values using different dielectric constants (see figure legend). The transition from short-distance interactions of the charge with its own mirror images ($-z \ll d$, slope = -1) to long-distance interactions ($-z \gg d$, slope = -2) is obvious.

13) and small Δ (Eq. 15) when the water dielectric constant ϵ_W is replaced by that of the membrane ϵ_M.

Introducing the hydration shell for the test charge leads to a finite difference of its zero point energies inside and outside the membrane. By entering a "pore" in the membrane, the ion must remove the "hydration shell" or at least parts of it. Because of the interaction of the ion with its own image charges, its energy lies below the total hydration energy. By using "effective hydration radii" one can account for the fact that the ion channel itself may contain water molecules and that the dielectric constant of water molecules tightly bound to an ion does not differ considerably from that of the hydrophilic protein side chains.

Fig. 5 *a* and *b*, displays the self energies of a unit charge using several dielectric constants and hydration radii. All distances are given relative to the membrane thickness *d*. The resulting energy must be divided by this parameter.

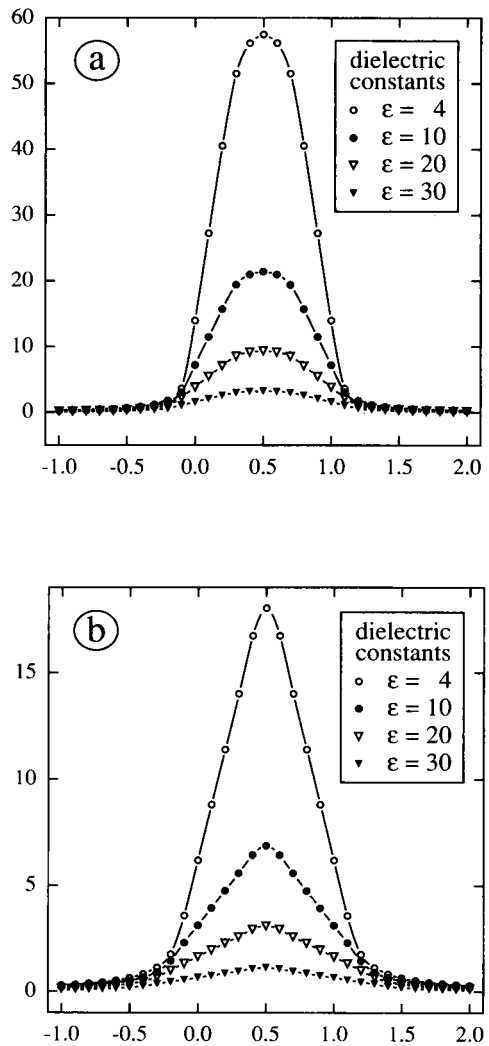

FIGURE 5 The self energy of an ion with unit charge and hydration radii of (*a*) $r_H = 0.1\ d$ and (*b*) $r_H = 0.2\ d$ at various dielectric constants (see figure legends).

Here, the calculation, of course, reproduces the well-known electrostatic barrier to penetration of an ion through the bilayer. Both the height and the slope of this barrier depend on the membrane dielectric constant ϵ_M and the hydration radius r_H.

The charge-charge interaction

The electrostatic interaction U_ν between a test charge q at $\mathbf{r}$ and a fixed charge Q_ν at $\mathbf{r}_\nu$ in the presence of the membrane can be put in the following general form:

$$U_\nu(\mathbf{r}, \mathbf{r}_\nu) = \frac{qQ_\nu}{\epsilon_k\|\mathbf{r} - \mathbf{r}_\nu\|} + \frac{qQ_\nu}{\epsilon_k}\mathcal{J}_\nu(\mathbf{r}, \mathbf{r}_\nu), \qquad (16)$$

with $\epsilon_1 = \epsilon_3 = \epsilon_W$ and $\epsilon_2 = \epsilon_M$. Numerical methods to calculate the integral $\mathcal{J}_\nu$ are discussed in detail in the Appendix (see Interaction with the Membrane Charges).

The first term describes the classic Coulomb interaction and the second one the polarization effect. To study the limiting behavior of the mirror images, it is useful to introduce $\tilde{r}$:

$$\tilde{r} = [(x - x_\nu)^2 + (y - y_\nu)^2 + (|z| + |z_\nu)^2]^{1/2}. \qquad (17)$$

In the case of sign $z = -\text{sign}\ z_\nu$, this quantity equals the distance between the two charges $\|\mathbf{r} - \mathbf{r}_\nu\|$.

As long as the fixed charge is placed inside the membrane, the limiting contribution from $\mathcal{G}_2$ can be described by a single mirror image:

$$\mathcal{J}_\nu\begin{pmatrix} z + z_\nu < d \\ 0 < z_\nu < d \end{pmatrix} \approx -\frac{\Delta}{\tilde{r}}\begin{cases} 1 & \text{for } \tilde{r} \ll d \\ \dfrac{2}{1+\Delta} & \text{for } \tilde{r} \gg d \end{cases}.$$

However, in the case of $z < 0$ and $z_\nu > 0$, the distance $\tilde{r}$ equals $\|\mathbf{r} - \mathbf{r}_\nu\|$, resulting in a simple Coulomb type of interaction. With $1 - 2\Delta/(1 + \Delta) = \epsilon_M/\epsilon_W$, this contribution from $\mathcal{G}_2$ accounts for the difference between ϵ_M and ϵ_W, leading to a limiting dielectric constant of ϵ_M.

The limiting dielectric constant for the interaction between the test charge far away from the membrane and a charge placed in the membrane is close to that of the solvent ϵ_W. The lowest order correction to the Coulomb law is given by

$$\mathcal{J}_\nu\begin{pmatrix} z_\nu < 0 \\ 0 < z < d \end{pmatrix} \approx +\frac{2\Delta[d - (1 + \Delta)z](|z| + |z_\nu|)}{\|\mathbf{r} - \mathbf{r}_\nu\|^3} \quad \text{for } \tilde{r} \gg d.$$

If both charges are outside the membrane and $\tilde{r}$ is large, the mirror images give rise to a charge-dipole interaction:

$$\mathcal{J}_\nu\begin{pmatrix} z < 0 \\ z_\nu < 0 \end{pmatrix} \approx +\frac{\Delta}{\tilde{r}}\begin{cases} 1 & \text{for } \tilde{r} \ll d \\ \dfrac{2d\|z| + |z_\nu\|}{\tilde{r}^2} & \text{for } \tilde{r} \gg d \end{cases}$$

and for the third range:

$$\mathcal{G}_\nu\begin{pmatrix} z<0 \\ d<z_\nu \end{pmatrix} \approx -\frac{\Delta^2}{\tilde{r}}\begin{cases} 1 & \text{for } \tilde{r} \ll d \\ \dfrac{2d\|z\| + \|z_\nu\|}{\tilde{r}^2} & \text{for } \tilde{r} \gg d \end{cases}.$$

To obtain a qualitative understanding of the effect of the images on the charge-charge interaction, it is helpful to consider the dielectric screening factor $\epsilon_{scr}(\mathbf{r}, \mathbf{r}_\nu)$. The dielectric screening factor represents a measure of the dielectric screening between a pair of charges at $\mathbf{r}$ and $\mathbf{r}_\nu$ owing to the presence of the low dielectric material of the membrane. The dielectric screening factor has the form and the range of numerical values of an "effective dielectric constant." For the usual Coulomb law, the dielectric constant is calculated by the inverse of the product of the distance between two atoms and the Coulomb energy E_C:

$$\epsilon = \frac{1}{\|\mathbf{r} - \mathbf{r}_\nu\| E_C}.$$

Consequently the dielectric screening factor ϵ_{scr} is defined by

$$\epsilon_{scr} = \frac{1}{\|\mathbf{r} - \mathbf{r}_\nu\| \mathcal{G}_k(\mathbf{r}, \mathbf{r}_\nu)} = \frac{\epsilon_k}{1 + \|\mathbf{r} - \mathbf{r}_\nu\| \mathcal{G}(\mathbf{r}, \mathbf{r}_\nu)} \tag{18}$$

with

$$\epsilon_k = \begin{cases} \epsilon_M & \text{for } 0 < z_\nu < d \\ \epsilon_W & \text{else} \end{cases}.$$

The results are given in Fig. 6 for three different positions of one of the two charges. The most simple situation is shown in Fig. 6 *a*, where one charge is placed in the middle of the membrane at *d*/2. The dielectric screening increases with increasing distance from the membrane value ϵ_M to the limiting value ϵ_W of the bulk solution. The increase in screening is much slower in the direction of the membrane. Two charges embedded in a low-dielectric membrane of finite thickness experience the dielectric constant of the solvent, if their distance $\|\mathbf{r} - \mathbf{r}_\nu\|$ is large compared to the membrane thickness *d*.

Interesting new features appear if the fixed charge is placed close to one of the two boundaries (say S_1). Again, at sufficient large distances the dielectric screening approaches that of the solvent. But in the asymmetric case (Fig. 6, *b* and *c*), the screening in the intermediate range may even excel that of the solvent. Charges in the vicinity of the boundary S_1 are screened more effectively from charges close to S_2 compared to bulk solution. Thus, the effect of the low dielectric membrane is not only to decrease the dielectric screening factor below that of the solvent. In certain regions it also increases the screening compared to the bulk solution.

If two charges are close to the membrane with a distance not large compared to the membrane thickness *d* (i.e., $|z| + |z_\nu| \ll \|\mathbf{R} - \mathbf{R}_\nu\| < d$), their dielectric screening factor ϵ_{scr} is close to one-half of the water dielectric constant. This value is found for two charges close to the boundary of two semiinfinite regions with dielectric constants of ϵ_M and ϵ_W (Jackson, 1962).

Such maps of the dielectric screening factor were calculated for several membrane dielectric constants ϵ_M (data not shown). As expected, the numerical values change considerably if the membrane dielectric constant changes; the overall qualitative behavior, however, was very similar to that shown in Fig. 6. The membrane dielectric constant influences the energy of the ions; the form of the barrier and charge-charge interaction remains virtually identical.

Dielectric polarization effects lead to a renormalization of the self energy and the Coulomb interaction. Therefore, a consistent theory based on heterogeneous dielectric regions

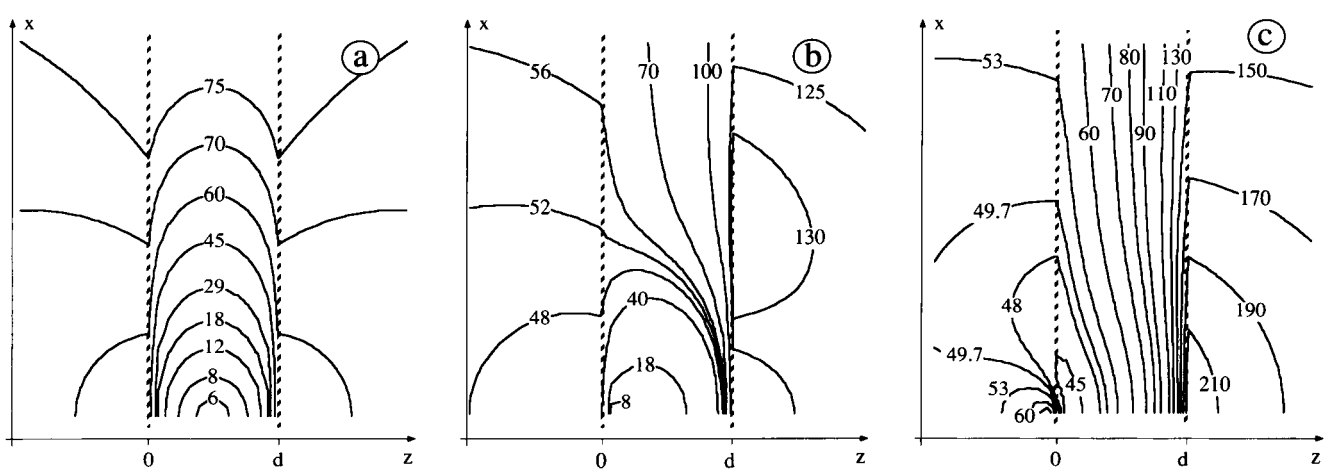

FIGURE 6 The dielectric screening factor ϵ_{scr} (see text) as a function of the position of the test charge $\mathbf{r} = (x, 0, z)$ with a fixed charge being placed (*a*) in the middle of the membrane at $z_\nu = d/2$, (*b*) inside the membrane close to the membrane surface at $z_\nu = d/10$, and (*c*) inside the solution close to the membrane surface at $z_\nu = -d/10$. The dielectric constant of the membrane is $\epsilon_M = 5$, and that of the solvent is $\epsilon_W = 80$. The lines of constant dielectric screening factor ϵ_{scr} are chosen to obtain a relatively regular spacing. It is indicated at the respective contour lines. The membrane extends from $z = 0$ to $z = d$ (see Fig. 1).

(e.g., for membranes, in proteins) should account for both renormalizations. This is, unfortunately, not the case with practically all treatments published to date (e.g., Poisson-Boltzmann, etc.), where the renormalization of the pair interaction is not considered. In contrast, the Green's functions approach presented here deals with this problem in a direct and accurate way.

Application to a molecular model of an ion channel

In this section the Green's function formalism is applied to an atomic model of the acetylcholine receptor channel (Hille, 1992; von Kitzing, 1995) to see the effect of the Green's formalism and to compare the result to more commonly used methods to calculate electrostatic interaction. It should be noted that it is considered as an illustrative example and not as a comprehensive study of the energetics of an ion passing the acetylcholine receptor channel.

The acetylcholine receptor channel is formed of five highly homologous subunits with the stoichiometry of α_2, β, γ, and δ (Akabas et al., 1994; Karlin, 1991; Unwin, 1993, 1995). Based on the change in ion conductivity resulting from point mutation experiments, the M2 segments in these subunits are assumed to align the narrow part of the channel pore (Akabas et al., 1994; Changeux, 1990; Charnet et al., 1990; Imoto et al., 1986, 1988, 1991; Konno et al., 1991; Leonard et al., 1988; Villarroel and Sakmann, 1992). Therefore, the channel model consists only of the M2 segments of the channel protein. Close to the narrowest part of the pore there is a ring of negative charges attracting anions into this region (Imoto et al., 1988; Konno et al., 1991).

Model building of the acetylcholine receptor channel

The M2 segment is assumed to consist of five linear α-helices. This assumption is not in agreement with recent results obtained from cryoelectron microscopic data (Unwin, 1995) for this channel. The model can be used, however, to study ion channels with charged amino acids close to the channel constriction.

The helices were packed densely around the threonine ring, which is assumed to form the channel constriction (Villarroel and Sakmann, 1992). The α-helices open toward the C-terminal side of the M2 segment (Changeux, 1990) by 10°. The orientation of the helices is such that the threonine ring and the two adjacent serine rings (Charnet et al., 1990) point into the channel lumen. This leads to a left-handed screw of the α-helices. The dihedral angle between the helices and the channel axis is 20°. The distance of the helix axis at the level of the threonine ring from the channel axis is 0.7 nm. For more details see von Kitzing (1995). (The coordinates of the model are available via WWW (http://sunny.mpimf-heidelberg.mpg.de/people/vkitzing/Eberhard.html).)

Calculating the energy profile of a test ion

The built structure was optimized according to the AMBER 3.0a force field by means of several annealing steps using molecular dynamic runs and finally using conjugated gradients. Such annealing steps are important for avoiding considerable conformation changes when calculating the energy profile for the ion. Because a large portion of the channel protein is missing, the model cannot expected to be stable on its own. Therefore, harmonic constraints are applied to the backbone atoms; a force constant of 1 kcal

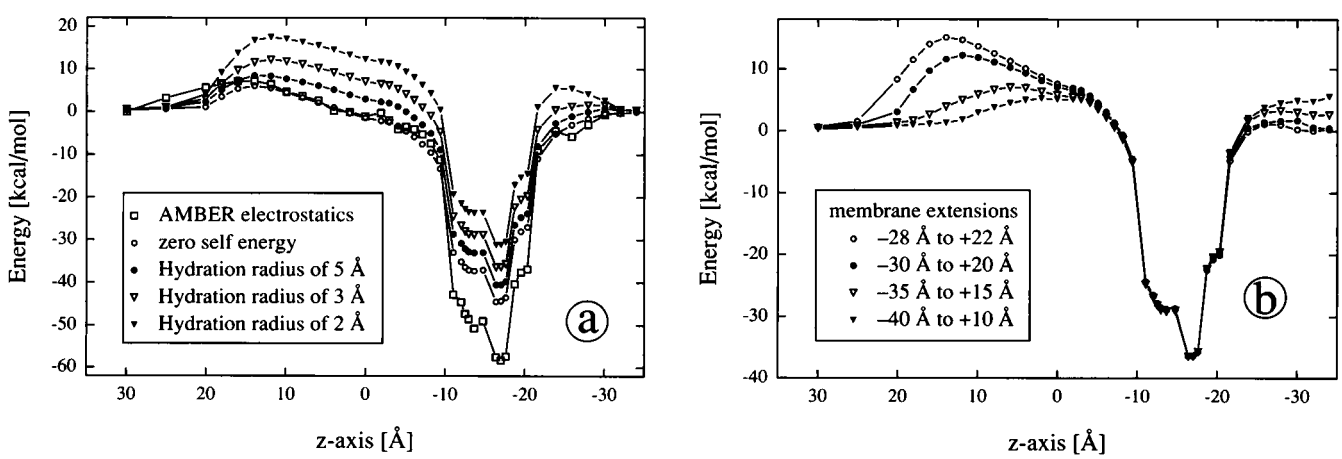

FIGURE 7 The charges and partial charges of a protein may reduce or even overcome the self energy seen by the ion due to the low dielectric membrane phase. This figure shows the "solvation" of the ion due to the protein using an atomic model for the acetylcholine receptor channel (see text). (*a*) The electrostatic energy of the AMBER program package using a distant dependent dielectric constant of $\epsilon = 2r$, the electrostatic interaction of the ion with the screened protein charges, and the complete ion-protein-membrane interaction, using different effective hydration radii (see figure legend), are given. The membrane extends from −30 Å to 20 Å. (*b*) The electrostatic interaction of the ion with the protein and membrane using an effective ionic hydration radius of 3 Å. The position of the membrane with respect to the channel model is shifted (see figure legend).

mol^{-1} $Å^2$ was used for the C_α atoms and 0.01 kcal mol^{-1} $Å^2$ for the remaining backbone atoms.

Fig. 7 shows the electrostatic energy of the ion as a function of its path through the channel. At every point the structure of the channel with the ion harmonically constrained to its initial position was energetically optimized by means of the AMBER dynamic annealing and conjugated gradient minimization (Singh et al., 1989; Weiner et al., 1984). Thus, the protein side chains were allowed to relax and to reorient freely in the electric field of the ion. A force constant of 5 kcal/(mol $Å^2$) for the ion allowed some flexibility in the ionic path but kept the ion sufficiently close to its starting point. Explicit water molecules were not included in the calculation.

Electrostatic energy profiles

In Fig. 7 *a* the electric energies are shown as calculated by the AMBER program package, using a distant dependent dielectric constant of $2r$ and a cutoff at 12 Å, the interaction of the ion with the screened protein charges (zero self energy), and the energy of the ion with effective hydration radii of 5 Å, 3 Å, and 2 Å. Although the dielectric constant of $2r$ provides rather strong dielectric screening, the electrostatic energy close to the negatively charged intermediate ring (−10 Å to −20 Å) is overestimated by one-third. In the range of −7 Å to 15 Å, the AMBER electrostatic energy compares reasonably well with the screened interaction energy. It is again higher then the latter. Setting the dielectric constant proportional to the distance between the charges r is an ad hoc, widely used assumption with absolutely obscure origin. In spite of the (probably accidental) qualitative similarity between this approximation and the exact treatment of the electrostatic field, we do not recommend its use in general.

To see the influence of the position of the membrane on short-range electrostatic interactions, the position of the membrane with respect to the model is shifted, leaving the thickness of 50 Å of the membrane constant. These results are shown in Fig. 7 *b*, indicating that short-range electrostatic interactions are nearly independent of the position of the membrane.

Comparison of these results with those for the bilayer electrostatic barrier (Fig. 5, *a* and *b*) shows that placement of protein charged groups in the membrane completely changes the latter in an asymmetric, structure-dependent way. Furthermore, the energy profile depends on the hydration radius r_H of the ion.

Consequences for ion permeation

The energies shown in Fig. 7 appear rather large when compared to those obtained from fitting rate models to experimental current-voltage data (Konno et al., 1991). The barrier at 10 Å (see Fig. 7 *a*) with a height between 10 and 20 kcal/mol results from electrostatic interactions with positively charged amino acids in the extracellular ring known to be rather influential on the ionic conductance (Konno et al., 1991). The strong binding energy at −18 Å between −20 and −60 kcal/mol is determined by negative charges in the intermediate and intracellular rings. Such large energies, however, are common for ion channel simulations that include charged amino acid side chains (Eisenman et al., 1990; Furois-Corbin and Pullman, 1991). With commonly used rate models in mind (Cooper et al., 1985; Eyring et al., 1949; Hille, 1992; Kramers, 1940), one would expect that the ion would enter the channel and only in rare cases leave it again.

Ion channels are in contact with electrolyte solutions. The positive charge in the extracellular ring would be screened by anions reducing this barrier height. The strong electric fields of the negative charges in the intracellular and intermediate rings would attract respective numbers of cations, creating an opposite electric field of the same order of magnitude as that of the two rings. This situation results in the breakdown of the constant field approximation and makes the use of barrier models obsolete for such highly charged ion channels (Eisenberg, 1996a,b).

CONCLUDING REMARKS

The method discussed in this article makes it possible to treat computationally expensive long-range dielectric polarization effects in the electrostatics of membrane-bound proteins and their interactions with charged solvent components (ions, ligands, etc.) in a straightforward manner. It is computationally robust and therefore can be easily incorporated in computer simulations and theories of ionic transport, binding equilibria, etc. This is in sharp contrast to methods involving the numerical solution of partial differential or integral equations (e.g., solving the Poisson or Poisson-Boltzmann approach numerically).

APPENDIX

In this appendix we discuss the computational procedures used to calculate the Green's functions of the main text (Eqs. 5, 6, and 7) with sufficient accuracy.

The numerical integration procedure

The remaining integrals in the Green's functions representing the self energy and the interaction between a charge and the mirror images of other charges are generally not solvable explicitly. Therefore, numerical methods are introduced. For the class of integrals involved in this paper, a Gauss-Laguerre quadrature seems to be most appropriate. The introduction of a Gauss-Chebyshev quadrature has proved to be less satisfactory (for further information see Overcoming the Oscillation Problem, below). For the Gauss-Laguerre type of numerical quadrature, the integral has to be brought into the standard form:

$$I = \int_0^\infty f(a)e^{-a}\,da. \tag{A1}$$

The function $f(a)$ should be sufficiently "well behaved" such that f must be presentable as a polynomial of sufficient low order (for details see Press et al., 1992, pp. 121). Therefore, substitutions must be found that cast the integrals into this form and ensure a well-behaved $f(a)$.

The following identity, which involves the geometric series, is used in several instances to improve the numerical behavior of the function $f(a)$ in Eq. A1:

$$\frac{1}{1-\Delta^2 e^{-\alpha a}} = 1 + \frac{\Delta^2 e^{-\alpha a}}{1-\Delta^2 e^{-\alpha a}} \tag{A2}$$

$$= \left(\sum_{\mu=0}^{n-1} \Delta^{2\mu} e^{-\mu\alpha a}\right) + \frac{\Delta^2 e^{-n\alpha a}}{1-\Delta^2 e^{-\alpha a}}.$$

The integration of the self energy

Outside the membrane ($z < 0$), the self energy function ϕ_S obtained from the Green's function $\mathcal{G}_1$ of region 1 was given by Eq. 6 by identifying $\mathbf{R}'$ with $\mathbf{R}$ and z' with z and neglecting the infinite vacuum self energy. This yields

$$\phi_S(z<0) = 2\int_0^\infty \Delta \exp(2kz)\frac{1-\exp(-2kd)}{1-\Delta^2\exp(-2kd)}\,dk$$

$$= -\frac{\Delta}{z}\int_0^\infty e^{-a}\frac{1-e^{-\alpha a}}{1-\Delta^2 e^{-\alpha a}}\,da \tag{A3}$$

$$= -\frac{\Delta}{z}\left[1 - \frac{1}{1+\alpha} + \frac{\Delta^2}{1+\alpha}\int_0^\infty e^{-a'}\frac{1-e^{-\alpha' a'}}{1-\Delta^2 e^{-\alpha' a'}}\,da'\right],$$

with

$$a = -2kz; \quad \alpha = -\frac{d}{z}; \quad a' = 1+\alpha a \quad \alpha' = \frac{\alpha}{1+\alpha}.$$

For $\alpha \gg 1$, the function $[1 - e^{-\alpha a}]/[1 - \Delta^2 e^{-\alpha a}]$ approaches its limiting value of 1 very rapidly; therefore the numerical integration becomes inaccurate. This difficulty can be removed by substituting α'.

Inside the membrane in the range of $0 < z \leq d/2$, the self energy becomes

$$\phi_S\left(0<z<\frac{d}{2}\right)$$

$$= -2\int_0^\infty \frac{\Delta\exp(-2kz) + \Delta\exp(-2k(d-z)) - 2\Delta^2\exp(-2kd)}{1-\Delta^2\exp(-2kd)}\,dk \tag{A4}$$

$$= -\frac{\Delta}{z}\int_0^\infty e^{-a}\frac{1+e^{-\beta a} - 2\Delta e^{-\gamma a}}{1-\Delta^2 e^{-\alpha a}}\,da,$$

with

$$a = 2kz; \qquad \alpha = \frac{d}{z}; \qquad \beta = \alpha - 2; \quad \text{and} \quad \gamma = \alpha - 1.$$

For numerical calculation the same procedure as above ensures $\alpha' < 1$, $\beta' < 1$, and $\gamma' < 1$.

Interaction with the membrane charges

The Green's functions $\mathcal{G}_1$, $\mathcal{G}_2$, and $\mathcal{G}_3$ from Eqs. 6, 5, and 7 can be combined into a single function:

$$\mathcal{G}_k(\mathbf{r}, \mathbf{r}_\nu) = \frac{1}{\epsilon_k\|\mathbf{r}-\mathbf{r}_\nu\|} + \frac{1}{\epsilon_k}\mathcal{J}_\nu, \tag{A5}$$

with $\epsilon_1 = \epsilon_3 = \epsilon_W$ and $\epsilon_2 = \epsilon_M$. The integral $\mathcal{J}_\nu$ is then given by the general form

$$\mathcal{J}_\nu\int_0^\infty \frac{J_0(k\|\mathbf{R}-\mathbf{R}_\nu\|)}{1-\Delta^2\exp(-2kd)}\{-\Delta\,\mathrm{sgn}(z_\nu)\exp[-k(|z|+|z_\nu|)]$$

$$+\Delta^2\,\mathrm{sgn}(d-z_\nu)\exp[-k(|d-z|+|d-z_\nu|)] \tag{A6}$$

$$+\Delta^2\,\mathrm{sgn}(d-z_\nu)\exp[-k(|z|+|d-z_\nu|+d)]\}\,dk.$$

To obtain working formulae for $\mathcal{J}_\nu$, one must consider six different cases, i.e., $z < 0$ and $0 < z < d$ in conjunction with $z_\nu < 0$, $0 < z_\nu < d$, and $d < z_\nu$. In the case $z < 0$ and $0 < z_\nu < d$, Eq. A6 becomes

$$\mathcal{J}_\nu\left(\begin{matrix} z<0 \\ 0<z_\nu<d\end{matrix}\right) = \int_0^\infty \frac{J_0(k\|\mathbf{R}-\mathbf{R}_\nu\|)}{1-\Delta^2\exp(-2kd)}$$

$$\{-\Delta\exp[-k(z_\nu - z)] + \Delta^2\exp[-k(2d+z_\nu - z)]$$

$$-\Delta\exp[-k(2d - z_\nu - z)]$$

$$+\Delta^2\exp[-k(2d - z_\nu - z)]\}\,dk.$$

The following substitution is introduced:

$$a = k(z_\nu - z) \Rightarrow k = \frac{a}{z_\nu - z}.$$

Thus for $z < 0$, the integral $\mathcal{J}_\nu$ becomes

$$\mathcal{J}_\nu\left(\begin{matrix} z<0 \\ 0<z_\nu<d\end{matrix}\right) = \frac{1}{z_\nu - z}\mathcal{T}_\nu,$$

with

$$\mathcal{T}_\nu = \int_0^\infty J_0(\beta a)\frac{-\Delta + \Delta^2 e^{-\gamma_1 a} - \Delta e^{-\gamma_2 a} + \Delta^2 e^{-\gamma_3 a}}{1-\Delta^2 e^{-\alpha a}} e^{-a}\,da \tag{A7}$$

and

$$\alpha = \frac{2d}{z_\nu - z}; \qquad \beta = \frac{\|\mathbf{R}-\mathbf{R}_\nu\|}{z_\nu - z}; \qquad \gamma_1 = \alpha; \tag{A8}$$

$$\gamma_2 = 2\frac{d - z_\nu}{z_\nu - z}; \qquad \text{and} \quad \gamma_3 = \gamma_2.$$

Next, the case is considered where the charge lies inside the membrane. Equation A6 then becomes

$$\mathcal{J}_\nu\begin{pmatrix}0<z<d\\0<z_\nu<d\end{pmatrix} = \int_0^\infty \frac{J_0(k\|\mathbf{R}-\mathbf{R}_\nu\|)}{1-\Delta^2\exp(-2kd)}\{-\Delta\exp[-k(z+z_\nu)] + \Delta^2\exp[-k(2d-z+z_\nu)] - \Delta\exp[-k(2d-z-z_\nu)] + \Delta^2\exp[-k(2d+z-z_\nu)]\}\,dk.$$

For numerical integration two cases have to be considered for $0<z<d$: $d>z+z_\nu$ and $d\le z+z_\nu$:

$$a=\begin{cases}k(z+z_\nu) & \text{for } d>z+z_\nu\\ k(z+z_\nu-2d) & \text{for } d\le z+z_\nu\end{cases}$$

$$\Rightarrow k=\begin{cases}\dfrac{a}{z+z_\nu} & \text{for } d>z+z_\nu\\ \dfrac{a}{2d-z-z_\nu} & \text{for } d\le z+z_\nu\end{cases}$$

Thus for $0<z<d$ and $d>z+z_\nu$, the integral $\mathcal{J}_\nu$ becomes

$$\mathcal{J}_\nu\begin{pmatrix}0<z<d\\d>z+z_\nu\end{pmatrix}=\frac{1}{z+z_\nu}\mathcal{T}_\nu, \tag{A9}$$

with

$$\alpha=\frac{2d}{2+z_\nu},\quad \beta=\frac{\|\mathbf{R}-\mathbf{R}_\nu\|}{z+z_\nu}\quad\text{and}\quad \gamma_1=2\frac{d-z}{z+z_\nu},\ \gamma_2=2\frac{d-z-z_\nu}{z+z_\nu},\ \gamma_3=2\frac{d-z_\nu}{z+z_\nu}. \tag{A10}$$

For $0<z<d$ and $d\le z+z_\nu$, the integral $\mathcal{J}_\nu$ becomes

$$\mathcal{J}_\nu\begin{pmatrix}0<z<d\\d\le z+z_\nu\end{pmatrix}=\frac{1}{2d-z-z_\nu}\mathcal{T}_\nu,$$

with

$$\alpha=\frac{2d}{2d-z-z_\nu},\quad \beta=\frac{\|\mathbf{R}-\mathbf{R}_\nu\|}{2d-z-z_\nu}\quad\text{and}\quad \gamma_1=2\frac{z}{2d-z-z_\nu},\ \gamma_2=2\frac{z+z_\nu-d}{2d-z-z_\nu},\ \gamma_3=2\frac{z_\nu}{2d-z-z_\nu}. \tag{A11}$$

For all three cases, $(z<0)\wedge(0<z_\nu<d)$, $(0<z<d)\wedge(d>z+z_\nu)$, and $(0<z<d)\wedge(d\le z+z_\nu)$, where at least one charge is located in the membrane, the general form of $\mathcal{T}_\nu$ in Eq. A7 does not change, only the respective values for the α, β, and γ's do. Because the energy must be conserved, the case of $(z<0)\wedge(0<z_\nu<d)$ equals the case $(0<z<d)\wedge(z_\nu<0)$. There are two additional situations not yet considered: $(z<0)\wedge(z_\nu<0)$ and $(z<0)\wedge(d<z_\nu)$. For $(z<0)\wedge(z_\nu<0)$ the integral $\mathcal{J}_\nu$ for the Green's function A6 becomes

$$\mathcal{J}_\nu\begin{pmatrix}z<0\\z_\nu<0\end{pmatrix}=\int_0^\infty\frac{J_0(k\|\mathbf{R}-\mathbf{R}_\nu\|)}{1-\Delta^2\exp(-2kd)}\{+\Delta\exp[+k(z+z_\nu)] - \Delta^2\exp[-k(2d-z-z_\nu)] - \Delta\exp[-k(2d-z-z_\nu)] + \Delta^2\exp[-k(2d-z-z_\nu)]\}\,dk.$$

The substitution required for numerical integration is given by

$$a=-k(z+z_\nu)\Rightarrow k=-\frac{a}{z+z_\nu}.$$

Thus, $\mathcal{J}_\nu$ becomes

$$\mathcal{J}_\nu\begin{pmatrix}z<0\\z_\nu<0\end{pmatrix}=-\frac{\Delta}{z+z_\nu}\int_0^\infty e^{-a}J_0(\beta a)\frac{1-e^{-\alpha a}}{1-\Delta^2e^{-\alpha a}}\,da, \tag{A12}$$

with

$$\alpha=\frac{2d}{|z+z_\nu|}\quad\text{and}\quad\beta=\frac{\|\mathbf{R}-\mathbf{R}_\nu\|}{|z+z_\nu|}.$$

For $(z<0)\wedge(d<z_\nu)$, Eq. A6 becomes

$$\mathcal{J}_\nu\begin{pmatrix}z<0\\d<z_\nu\end{pmatrix}=\int_0^\infty\frac{J_0(k\|\mathbf{R}-\mathbf{R}_\nu\|)}{1-\Delta^2\exp(-2kd)}\{-\Delta\exp[-k(z_\nu-z)] + \Delta^2\exp[-k(2d+z_\nu-z)] + \Delta\exp[-k(z_\nu-z)] - \Delta^2\exp[-k(z_\nu-z)]\}\,dk.$$

The substitution required for numerical integration is given by

$$a=k(z_\nu-z)\Rightarrow k=\frac{a}{z_\nu-z}.$$

Thus, $\mathcal{J}_\nu$ becomes

$$\mathcal{J}_\nu\begin{pmatrix}z<0\\d<z_\nu\end{pmatrix}=-\frac{\Delta^2}{z_\nu-z}\int_0^\infty e^{-a}J_0(\beta a)\frac{1-e^{-\alpha a}}{1-\Delta^2e^{-\alpha a}}\,da, \tag{A13}$$

with

$$\alpha=\frac{2d}{z_\nu-z}\quad\text{and}\quad\beta=\frac{\|\mathbf{R}-\mathbf{R}_\nu\|}{z_\nu-z}.$$

There is another case, which is only of theoretical importance as a test for self-consistency $(0<z<d)\wedge(z_\nu<0)$:

$$\mathcal{J}_\nu\begin{pmatrix}0<z<d\\z_\nu<0\end{pmatrix}=\int_0^\infty\frac{J_0(k\|\mathbf{R}-\mathbf{R}_\nu\|)}{1-\Delta^2\exp(-2kd)}\{+\Delta\exp[-k(z-z_\nu)]$$

$$- \Delta^2 \exp[-k(2d - z - z_\nu)]$$
$$- \Delta \exp[-k(2d - z - z_\nu)]$$
$$+ \Delta^2 \exp[-k(2d + z - z_\nu)]\} \, dk.$$

The substitution required for numerical integration is given by

$$a = k(z - z_\nu) \Rightarrow k = \frac{a}{z - z_\nu}$$

$$\mathcal{J}_\nu\begin{pmatrix} 0 < z < d \\ z_\nu < 0 \end{pmatrix} = \frac{1}{z - z_\nu} \mathcal{T}_\nu,$$

with

$$\mathcal{T}_\nu = \int_0^\infty J_0(\beta a) \frac{+\Delta - \Delta^2 e^{-\gamma_1 a} - \Delta e^{-\gamma_2 a} + \Delta^2 e^{-\gamma_3 a}}{1 - \Delta^2 e^{-\alpha a}} e^{-a} \, da$$

and

$$\alpha = \frac{2d}{z - z_\nu}; \qquad \beta = \frac{\|\mathbf{R} - \mathbf{R}_\nu\|}{z - z_\nu}; \qquad \gamma_1 = 2\frac{d - z_\nu}{z - z_\nu};$$
$$\gamma_2 = \gamma_1; \quad \text{and} \quad \gamma_3 = \alpha.$$

Overcoming the oscillation problem

The integrals for the self energy in Eqs. A3 and A4 can easily be computed by means of a 15-point Gauss-Laguerre integration. The same procedure also works in the case of charge-charge interaction as long as $|z| + |z_\nu|$ is considerably larger than $\|\mathbf{R} - \mathbf{R}_\nu\|$ and thus β (Eqs. A8, A10, and A11) remains small. For $\beta \gg 1$, the strong oscillations of the Bessel function J_0 require considerably more points for integration.

By means of the substitution $a = \ln y$, the interval of the integration reduces to [0, 1]. Thus a Gauss-Chebyshev integration could be introduced. For this method, the formulae for any number of points are known. For the integration of the self energy, the Gauss-Chebyshev integration required about 1000 points for similar accuracy compared with the 15-point Gauss-Laguerre integration. In the case of the charge interaction integral, the number of points required for reasonable accuracy was about $n = 10\beta$. Thus for large β (small $|z| + |z_\nu|$ and large $\|\mathbf{R} - \mathbf{R}_\nu\|$), the time for integration would become prohibitively long.

The problem of integrating the charge interaction energy has been solved by means of the geometric series of the denominator in the integral A2. Substitution into A7 leads to

$$\mathcal{T}_\nu = \int_0^\infty J_0(\beta a) \frac{f(\gamma_1, \gamma_2, \gamma_3)}{1 - \Delta^2 e^{-\alpha a}} e^{-a} \, da \tag{A14}$$

$$= \left(\sum_{\mu=0}^{n-1} \frac{\Delta^{2\mu}}{1 + \mu\alpha} K_{\nu\mu}^{\text{int}} \right) + \frac{\Delta^{2n}}{1 + n\alpha} L_{\nu n}^{\text{int}},$$

with

$$f(\gamma_1, \gamma_2, \gamma_3) = -\Delta + \Delta^2 e^{-\gamma_1 a} - \Delta e^{-\gamma_2 a} + \Delta^2 e^{-\gamma_3 a}$$

$$\alpha_n = \frac{\alpha}{1 + n\alpha}; \qquad \beta_n = \frac{\beta}{1 + n\alpha}$$

$$\text{and} \quad \gamma_{kn} = \frac{\gamma_k}{1 + n\alpha} \quad \text{with} \quad k \in \{1, 2, 3\},$$

and

$$K_{\nu\mu}^{\text{int}} = \int_0^\infty J_0(\beta a) f(\gamma_{1\mu}, \gamma_{2\mu}, \gamma_{3\mu}) e^{-a} \, da$$

$$= \sum_{\kappa=1}^{4} \frac{\lambda_\kappa}{1 + \gamma_{\kappa\mu}} \frac{1}{[1 + (\beta_\mu / 1 + \gamma_{\kappa\mu})^2]^{1/2}} \tag{A15}$$

$$\lambda_2 = \lambda_4 = -\Delta; \qquad \lambda_1 = \lambda_3 = \Delta^2; \quad \text{and} \quad \gamma_{4\mu} = 0.$$

$$L_{\nu n}^{\text{int}} = \int_0^\infty J_0(\beta_n a) \frac{f(\gamma_{1n}, \gamma 2_n, \gamma_{3n})}{1 - \Delta^2 e^{-\alpha_n a}} e^{-a} \, da.$$

Although the analytical form of the integral $L_{\nu n}^{\text{int}}$ remaining to be solved is the same as the original one (Eq. A14), the value of β_n has changed:

$$\beta_n = \frac{\beta}{1 + n\alpha} \overset{(A8)}{=} \frac{\|\mathbf{R} - \mathbf{R}_\nu\|}{|z - z_\nu| + 2n\alpha}.$$

A similar equation holds for the cases where $z > 0$. Thus Eq. A15 can be computed using the 15-point Gauss-Laguerre quadrature with reasonable accuracy if the following relation holds:

$$\|\mathbf{R}\nu - \mathbf{R}_\nu\| < |z - z_\nu| + 2nd.$$

The same procedure also works in the case where the two considered charges are outside the membrane. In this case $K_{\nu\mu}$ and $L_{\nu\mu}$ have to be calculated as

$$K_{\nu\mu}^{\text{ext}} = \int_0^\infty J_0(\beta_\mu a)(1 - e^{-\alpha_\mu a}) e^{-a} da$$

$$= \frac{1}{[1 + \beta_\mu]^{1/2}} - \frac{1}{1 + \alpha_\mu} \frac{1}{[1 + (\beta_\mu / 1 + \alpha_\mu)]^{1/2}}$$

and

$$L_{\nu n}^{\text{ext}} = \int_0^\infty J_0(\beta_n a) \frac{1 - e^{-\alpha_n a}}{1 - \Delta^2 e^{-\alpha_n a}} e^{-a} \, da.$$

Limiting formulas for the charge-charge interaction

Whereas the limiting behavior of the self energy potential function ϕ_S was relatively easy to calculate, the limits for the mirror images of the charge-charge interactions require a few thoughts. Three limits are of major interest: 1) both charges are close to the wall $|z| + |z_\nu| \ll d$; 2) both charges are remote from the walls $|z| + |z_\nu| \gg d$; and 3) the charges include a large distance along the walls $\|\mathbf{R} - \mathbf{R}_\nu\| \gg d$. The limits have to be obtained for only two forms of the integral $\mathcal{T}_\nu$: 1) $\mathcal{T}_A$ from Eq. A7 and 2) $\mathcal{T}_B$ from the Eqs. A12 and A13. The coefficients in

the integral and the prefactors will change from case to case. The first case, 1), is considered:

$$\mathcal{T}_A = \int_0^\infty J_0(\beta a) \frac{-\Delta + \Delta^2 e^{-\gamma_{1a}} - \Delta e^{-\gamma_{2a}} + \Delta^2 e^{-\gamma_{3a}}}{1 - \Delta^2 e^{-\alpha a}} e^{-a}\, da.$$

One then obtains the limits:

$$\lim_{|z|+|z_\mu|/d\to 0} \mathcal{T}_A = -\Delta \int_0^\infty J_0(\beta a) e^{-a}\, da = -\frac{\Delta}{[1+\beta^2]^{1/2}}$$

$$\lim_{|z|+|z_\mu|/d\to \infty} \mathcal{T}_A = -\frac{2\Delta}{1+\Delta} \int_0^{170} J_0(\beta a) e^{-a}\, da$$

$$= -\frac{2\Delta}{1+\Delta} \frac{1}{[1+\beta^2]^{1/2}}$$

$$\lim_{\|R-R_\mu\|/d\to\infty} \mathcal{T}_A = -\frac{2\Delta}{1+\Delta} \int_0^\infty J_0(\beta a)\, da = -\frac{2\Delta}{1+\Delta} \frac{1}{\beta}.$$

Interestingly, the limits for large $|z| + |z_\mu|$ and large $\|\mathbf{R} - \mathbf{R}_\mu\|$ are very similar. The other set of $\mathcal{T}$-integrals (Eqs. A12 and A13) are of the form

$$\mathcal{T}_B = \int_0^\infty J_0(\beta a) \frac{1 - e^{-\alpha a}}{1 - \Delta^2 e^{-\alpha a}} e^{-a}\, da.$$

The three limits yield

$$\lim_{|z|+|z_\mu|/d\to 0} \mathcal{T}_B = \int_0^\infty J_0(\beta a) e^{-a}\, da = \frac{1}{[1+\beta^2]^{1/2}}$$

$$\lim_{|z|+|z_\mu|/d\to \infty} \mathcal{T}_B = \alpha \int_0^\infty a J_0(\beta a) e^{-a}\, da = \frac{\alpha}{[1+\beta^2]^{3/2}}$$

$$\lim_{\|R-R_\mu\|/d\to\infty} \mathcal{T}_B = \alpha \int_0^\infty a J_0(\beta a)\, da = \frac{\alpha}{\beta^3}.$$

We thank Dr. Alfredo Villarroel for critically reading the manuscript. DMS acknowledges support by the BMFT (Bundesministerium für Forschung und Technologie, Germany).

REFERENCES

Akabas, M. H., C. Kaufmann, P. Archdeacon, and A. Karlin. 1994. Identification of acetylcholine-receptor channel-lining residues in the entire M2 segment of the α-subunit. *Neuron.* 13:919–927.

Aleman, C., M. Orozco, and F. J. Luque. 1994. Multicentric charges for the accurate representation of electrostatic interactions in force-field calculations for small molecules. *Chem. Phys.* 189:573–584.

Alvarez O., A. Villarroel, and G. Eisenman. 1992. Calculation of ion currents from energy profiles and energy profiles from ion currents in multibarrier, multisite, multioccupancy channel model. *Methods Enzymol.* 207:816–854.

Andersen, O. S., and R. E. Koeppe II. 1992. Molecular determinants of channel function. *Physiol. Rev.* 72:S89–S158.

Åqist, J., and A. Warshel. 1989a. Consistent calculations of electrostatic free energies in membrane channels. The solvation of Na^+ by the gramicidin channel. *Comm. Mol. Cell. Biophys.* 6:91–110.

Åqist, J., and A. Warshel. 1989b. Energetics of ion permeation through membrane channels: solvation of Na^+ by gramicidin A. *Biophys. J.* 56:171–182.

Bayley, C. I., P. Cieplak, W. D. Cornell, and P. A. Kollman. 1993. A well-behaved electrostatic potential based method using charge restraints for deriving atomic charges: the RESP model. *J. Phys. Chem.* 97:10269–10280.

Bek, S., and E. Jakobsson. 1994. Brownian dynamics study of a multiply-occupied cation channel: application to understanding permeation in potassium channels. *Biophys. J.* 66:1028–1038.

Bharadwaj, R., A. Windemuth, S. Sridharan, B. Honig, and A. Nicholls. 1995. The fast multipole boundary element method for molecular electrostatics—an optimal approach for large systems. *J. Comput. Chem.* 16:898–913.

Boiko, I. I. 1993. The Electron Gas Kinetic Due to the Interaction of the Gas with the Fluctuating Potential (Russian). Nauka Dumka, Kiev.

Bopp, P. A., A. A. Kornyshev, and G. Sutmann. 1996. Static nonlocal dielectric function of liquid water. *Phys. Rev. Lett.* 76:1280–1283.

Born, M. 1920. Volumen und Hydratationswärme der Ionen. *Z. Phys.* 1:45–48.

Cafiso, D. S. 1994. Alamethicin—a peptide model for voltage gating and protein membrane interactions. *Annu. Rev. Biophys. Biomol. Struct.* 23:141–165.

Changeux, J.-P. 1990. The nicotinic acetylcholine receptor: an allosteric protein prototype of ligand-gated ion channels. *Trends Pharmacol. Sci.* 11:485–491.

Charnet, P., C. Labarca, R. J. Leonard, N. Vogelaar, L. Czyzyk, A. Gouin, N. Davidson, and H. Lester. 1990. An open-channel blocker interacts with adjacent turns of α-helices in the nicotinic acetylcholine receptor. *Neuron.* 2:87–95.

Cooper, K., E. Jakobsson, and P. Wolynes. 1985. The theory of ion transport through membrane channels. *Prog. Biophys. Mol. Biol.* 46: 51–96.

Cornell, W. D., P. Cieplak, C. I. Bayly, I. R. Gould, K. M. Merz, D. M. Ferguson, D. C. Spellmeyer, T. Fox, J. W. Caldwell, and P. A. Kollman. 1995. A 2nd generation force-field for the simulation of proteins, nucleic acids, and organic molecules. *J. Am. Chem. Soc.* 117:5179–5197.

Cramer, C. J., and D. G. Truhlar. 1992. An SCF solvation model for the hydrophobic effect and absolute free energies of aqueous solvents. *Science.* 256:213–217.

Darden, T., D. York, and L. Pedersen. 1993. Particle mesh Ewald: an (*N* log *N*) method for Ewald sums in large systems. *J. Chem. Phys.* 98: 10089–10092.

Dilger, J. P., L. R. Fisher, and P. A. Haydon. 1982. A critical comparison of electrical and optical methods for bilayer thickness determination. *Chem. Phys. Lipids.* 30:159.

Dinur, U., and A. T. Hagler, 1989. Determination of atomic point charges and point dipoles from the Cartesian derivatives of the molecular dipole moment and second moments, and from energy second derivatives of planar dimers. (1) Theory. *J. Chem. Phys.* 91:2949–2970.

Dorman, V., M. B. Partenskii, and P. C. Jordan. 1996. A semimicroscopic Monte Carlo study of permeation energetics in a gramicidin-like channel—the origin of cation selectivity. *Biophys. J.* 70:121–134.

Dosen-Micovic, L., and N. L. Allinger. 1978. The effects of electrostatic interactions and solvation energies on conformational equilibria in dihalides and haloketones. *Tetrahedron.* 34:3385–3393.

Eisenberg, D., M. Wesson, and M. Yamashita. 1989. Interpretation of protein folding and binding with atomic solvation parameters. *Chim. Scripta.* 29A:217–221.

Eisenberg, R. S. 1996a. Atomic biology, electrostatics, and ionic channels. *In* New Developments and Theoretical Studies of Proteins. R. Elber, editor. World Scientific Publishing, Philadelphia.

Eisenberg, R. S. 1996b. Computing the field in proteins and channels. *J. Membr. Biol.* 150:1–25.

Eisenman, G., and O. Alvarez. 1991. Structure and function of channels and channelogs as studied by computational chemistry. *J. Membr. Biol.* 119:109–132.

Eisenman, G., A. Villarroel, M. Montal, and O. Alvarez. 1990. Energy profiles for ion permeation in pentameric protein channels: from viruses to receptor channels. *In* Progress in Cell Research. J. M. Ritchie, P. J. Magistretti, and L. Bolis, editors. Springer Verlag, New York. 195–211.

Eyring, H., R. Lumry, and J. W. Woodbury. 1949. Some applications of modern rate theory to physiological systems. *Rec. Chem. Prog.* 10: 100–114.

Furois-Corbin, S., and A. Pullman. 1991. The effect of point mutations on energy profiles in a model of the nicotinic acetylcholine receptor channel. *Biophys. Chem.* 39:153–159.

Hagler, A. T., and C. S. Ewig. 1994. On the use of quantum energy surfaces in the derivation of molecular force fields. *Comp. Phys. Commun.* 84:131–155.

Halgren, T. A. 1995. Potential energy functions. *Curr. Opin. Struct. Biol.* 5:205–210.

Harvey, S. C. 1989. Treatment of electrostatic effects in macromolecular modeling. *Proteins.* 5:78–92.

Hawkins, G. D., C. J. Cramer, and D. G. Truhlar. 1995. Pairwise solute descreening of solute charges from a dielectric medium. *Chem. Phys. Lett.* 246:122–129.

Hille, B. 1992. Ionic Channels of Exitable Membranes. Sinauer Associates, Sunderland, MA.

Holm, L., and C. Sander. 1992. Evaluation of protein models by atomic solvation preference. *J. Mol. Biol.* 225:93–105.

Hummer, G., L. R. Pratt, and A. E. Garcia. 1996. Free energy of ionic hydration. *J. Phys. Chem.* 100:1206–1215.

Hyun, J. K., C. S. Babu, and T. Ichiye. 1995. Apparent local dielectric response around ions in water—a method for its determination and its applications. *J. Phys. Chem.* 99:5187–5195.

Imoto, K., C. Busch, B. Sakmann, M. Mishina, T. Konno, J. Nakai, H. Bujo, Y. Mori, K. Fukuda, and S. Numa. 1988. Rings of negatively charged amino acids determine the acetylcholine receptor channel conductance. *Nature.* 335:645–648.

Imoto, K., T. Konno, J. Nakai, F. Wang, M. Mishina, and S. Numa. 1991. A ring of uncharged polar amino acids as a component of channel constriction in the nicotinic acetylcholine receptor. *FEBS Lett.* 289: 193–200.

Imoto, K., C. Methfessel, B. Sakmann, M. Mishina, Y. Mori, T. Konno, K. Fukuda, M. Kurasaki, H. Bujo, Y. Fujita, and S. Numa. 1986. Location of a δ-subunit region determining ion transport through the acetylcholine receptor channel. *Nature.* 324:670–674.

Jackson, J. D. 1962. Classical Electrodynamics. John Wiley, New York.

Jakobsson, E. 1993. Hierarchies of simulation methods in understanding biomolecular function. *Int. J. Quant. Chem.* 1993:25–36.

Jakobsson, E., and S.-W. Chiu. 1988. Application of Brownian motion theory to the analysis of membrane channel ionic trajectories calculated by molecular dynamics. *Biophys. J.* 54:751–756.

Jordan, P. C. 1981. Energy barriers for passage of ions through channels. Exact solution of two electrostatic problems. *Biophys. Chem.* 13: 203–212.

Jordan, P. C. 1982. Electrostatic modeling of ion pores. (1) Energy barriers and electric field profiles. *Biophys. J.* 39:157–164.

Jordan, P. C. 1983. Electrostatic modeling of ion pores. (2) Effects attributable to the membrane dipole potential. *Biophys. J.* 41:189–195.

Jordan, P. C. 1990. Ion-water and ion-polypeptide in a gramicidin-like channel: a molecular dynamics study. *Biophys. J.* 58:1133–1156.

Jordan, P. C. 1993. Interactions of ions with membrane proteins. *In* Thermodynamics of Membrane Receptors and Channels. M. B. Jackson, editor. CRC Press, Boca Raton, FL. 27–80.

Juffer, A. H., and H. J. C. Berendsen. 1993. Surface Boundary Conditions: A Simulation Model for Macromolecules. Springer-Verlag, Berlin, Heidelberg. 137–156.

Juffer, A. H., E. F. F. Botta, B. A. M. van Keulen, A. van der Ploeg, and H. J. C. Berendsen. 1991. The electric potential of a macromolecule in a solvent: a fundamental approach. *J. Comput. Phys.* 97:144–171.

Karlin, A. 1991. Explorations of the nicotinic acetylcholine receptor. *Harvey Lecture Ser.* 85:71 107.

Kerr, I. D., R. Sankararamakrishnan, O. S. Smart, and M. S. P. Sansom. 1994. Parallel helix bundles and ion channels—molecular modeling via simulated annealing and restrained molecular dynamics. *Biophys. J.* 67:1501–1515.

Kirkwood, J. G. 1934. Theory of solutions of molecules containing widely separated charges with special application to zwitterions. *J. Chem. Phys.* 2:351–361.

Konno, T., C. Busch, E. von Kitzing, K. Imoto, F. Wang, J. Nakai, M. Mishina, S. Numa, and B. Sakmann. 1991. Rings of anionic amino acids as structural determinants of ion selectivity in the acetylcholine receptor channel. *Proc. R. Soc. Lond. B.* 244:69–79.

Kornyshev, A. A., and G. Sutmann. 1996. The shape of the nonlocal dielectric function of polar liquids and the implications for thermodynamic properties of electrolytes—a comparative study. *J. Chem. Phys.* 104:1524–1544.

Kramers, H. A. 1940. Brownian motion in a field of force and the diffusion model of chemical reactions. *Physica.* 7:284–304.

Kuwajima, S., and A. Warshel. 1988. The extended Ewald method: a general treatment of long-range electrostatic interactions in microscopic simulations. *J. Chem. Phys.* 89:3751–3759.

Lavery, R., K. Zakrzewska, and A. Pullman. 1984. Optimized monopole expansions for the representation of the electrostatic properties of the nucleic acids. *J. Comput. Chem.* 5:363–373.

Lee, F. S., and A. Warshel. 1992. A local reaction field method for fast evaluation of long-range electrostatic interactions in molecular simulations. *J. Chem. Phys.* 97:3100–3107.

Leonard, R. J., C. G. Labarca, P. Chanet, N. Davidson, and H. A. Lester. 1988. Evidence that the M2 membrane-spanning region lines the ion channel pore of the nicotinic receptor. *Science.* 242:1578–1581.

Levitt, D. G. 1978a. Electrostatic calculations for an ion channel. (1) Energy and potential profiles and interactions between ions. *Biophys. J.* 22:209–219.

Levitt, D. G. 1978b. Electrostatic calculations for an ion channel. (2) Kinetic behaviour of the gramicidin A channel. *Biophys. J.* 22:219–247.

Levitt, D. G. 1991. General continuum theory for multi-ion channel. (2) Application to acetylcholine channel. *Biophys. J.* 59:278–288.

Luty, B. A., and W. F. van Gunsteren. 1996. Calculating electrostatic interactions using the particle-particle particle-mesh method with nonperiodic long-range interactions. *J. Phys. Chem.* 100:2581–2587.

Mahanty, J., and B. W. Ninham. 1976. Dispersion Forces. Academic Press, New York.

Mohan, V., M. E. Davis, J. A. McCammon, and B. M. Pettitt. 1992. Continuum model calculations of solvation free energies: accurate evaluation of electrostatic contributions. *J. Phys. Chem.* 96:6428–6431.

Oiki, S., V. Madison, and M. Montal. 1990. Bundles of amphipathic transmembrane α-helices as a structural motif for ion-conducting channel proteins: studies on sodium channels and acetylcholine receptors. *Proteins.* 8:226–236.

Parsegian, V. A. 1969. Energy of an ion crossing a low dielectric membrane: solutions to four relevant electrostatic problems. *Nature.* 221:844–846.

Parsegian, V. A. 1975. Ion-membrane interactions and structural forces. *Ann. N. Y. Acad. Sci.* 264:161–174.

Partenskii, M. B., M. Cai, and P. C. Jordan. 1991. A dipolar chain model for the electrostatics of transmembrane ion channels. *Chem. Phys.* 153: 125–131.

Partenskii, M. B., V. Dorman, and P. C. Jordan. 1994. Influence of a channel-forming peptide on energy barriers to ion permeation, viewed from a continuum dielectric perspective. *Biophys. J.* 67:1429–1438.

Partenskii, M. B., and P. C. Jordan. 1992a. Nonlinear dielectric behavior of water in transmembrane ion channels: ion energy barriers and channel dielectric constant. *J. Phys. Chem.* 96:3906–3910.

Partenskii, M. B., and P. C. Jordan. 1992b. Theoretical perspectives on ion-channel electrostatics—continuum and microscopic approaches. *Q. Rev. Biophys.* 25:477–510.

Pearlman, D. A., and S.-H. Kim. 1990. Atomic charges for DNA constituents derived from single-crystal X-ray diffraction data. *J. Mol. Biol.* 211:171–187.

Polymeropoulos, E. E., and J. Brickmann. 1985. Molecular dynamics of ion transport through transmembrane mode channels. *In* Annual Reviews in Biophysics and Biophysical Chemistry. D. M. Engelman, C. R. Cantor, and P. Thomas D, editors. 315–330.

Press, W. H., S. A. Teukolsky, W. T. Vetterling, and B. P. Fannery. 1992. Numerical Recipes in C. Cambridge University Press, Cambridge.

Reynolds, C. A., J. W. Essex, and W. G. Richards. 1992. Atomic charges for variable molecular conformations. *J. Am. Chem. Soc.* 114: 9075–9079.

Roux, B. 1993. Nonadditivity in cation peptide interactions—a molecular dynamics and ab initio study of Na^+ in the gramicidin channel. *Chem. Phys. Lett.* 212:231–240.

Roux, B., and M. Karplus. 1994. Molecular dynamics simulations of the gramicidin channel. *Annu. Rev. Biophys. Biomol. Struct.* 23:731–761.

Sancho, M., M. B. Partenskii, V. Dorman, and P. C. Jordan. 1995. Extended dipolar chain model for ion channels—electrostriction effects and the translocational energy barrier. *Biophys. J.* 68:427–433.

Sansom, M. S. P. 1993. Structure and function of channel-forming peptaibols. *Q. Rev. Biophys.* 26:365–421.

Schaefer, M., and M. Karplus. 1996. A comprehensive analytical treatment of continuum electrostatics. *J. Phys. Chem.* 100:1578–1599.

Schiffer, C. A., J. W. Caldwell, P. A. Kollman, and R. M. Stroud. 1993. Protein structure prediction with a combined solvation free energy-molecular mechanics force-field. *Mol. Simul.* 10:121.

Schreiber, H., and O. Steinhauser. 1992. Cutoff size does strongly influence molecular dynamics results on solvated polypeptides. *Biochemistry.* 31:5856–5860.

Sharp, K. 1991. Incorporating solvent and ion screening into molecular dynamics using the finite-difference Poisson-Boltzmann method. *J. Comput. Chem.* 12:454–468.

Sharp, K. A. 1993. Inclusion of solvent effects in molecular mechanics force fields. *In* Computer Simulations of Biomolecular Systems: Theoretical and Experimental Applications. W. F. van Gunsteren, P. K. Weiner, and A. J. Wilkinson, editors. ESCOM, Leiden. 147–160.

Shaw, P. B. 1985. Theory of the Poissons Green's function for discontinuous dielectric media with an application to protein biophysics. *Phys. Rev. A.* 32:2476–2487.

Simonson, T., D. Perahia, and A. T. Brünger. 1991. Microscopic theory of the dielectric properties of proteins. *J. Mol. Biol.* 218:859–886.

Singh, U. C., P. K. Weiner, J. Caldwell, and P. Kollman. 1989. AMBER 3.0 Revision A, Assisted Model Building with Energy Refinement. Department of Pharmaceutical Chemistry, School of Pharmacy, University of California, San Francisco, CA.

Sklenar, H., F. Eisenhaber, M. Poncin, and R. Lavery. 1990. Including solvent and counterion effects in the force fields of macromolecular mechanics: the field integrated electrostatic approach (FIESTA). *In* Theoretical Biochemistry and Molecular Biophysics. D. L. Beveridge, and R. Lavery, editors. Adenine Press, New York. 317–335.

Smythe, W. R. 1939. Static and Dynamic Electricity. McGraw-Hill, New York.

Soumpasis, D. M., M. Robert-Nicoud, and T. M. Jovin. 1987. B-Z DNA conformational transition in 1:1 electrolytes: dependence upon counterion size. *FEBS Lett.* 213:341–344.

Stakold, I. P. 1968. Boundary Value Problems of Mathematical Physics. Macmillan, New York.

Still, W. C., A. Tempczyk, R. C. Hawley, and T. Hendrickson. 1990. Semianalytical treatment of solvation for molecular mechanics and dynamics. *J. Am. Chem. Soc.* 112:6127–6129.

Stokes, R. H. 1964. The van der Waals radii of gaseous ions of the noble gas structure in relation to hydration energies. *J. Am. Chem. Soc.* 86:979–982.

Stouten, P. F. W., C. Froemmel, H. Nakamura, and C. Sander. 1993. An effective solvation term based on atomic occupancies for use in protein simulations. *Mol. Simul.* 10:97–120.

Syganow, A., and E. von Kitzing. 1995. The integral weak diffusion and diffusion approximations applied to ion transport through biological ion channels. *J. Phys. Chem.* 99:12030–12040.

Tlewelling, R. F., and W. L. Hubbel. 1986. The membrane dipole potential in a total membrane potential model. *Biophys. J.* 49:541–552.

Toyoshima, C., and N. Unwin. 1988. Ion channel of acetylcholine receptor reconstructed from images of postsynaptic membranes. *Nature.* 336: 247–250.

Tredgold, R. H., and P. N. Hole. 1976. Dielectric behaviour of dry synthetic polypeptides. *Biochim. Biophys. Acta.* 443:137–142.

Unwin, N. 1993. Nicotinic acetylcholine receptor at 9 Å resolution. *J. Mol. Biol.* 229:1101–1124.

Unwin, N. 1995. Acetylcholine-receptor channel imaged in the open state. *Nature.* 373:37–43.

van Gunsteren, W. F., and H. J. C. Berendsen. 1990. Computer simulation of molecular dynamics: methodology, applications, and perspectives in chemistry. *Angew. Chem. Int. Ed. Engl.* 29:992–1023.

Veresov, V. G. 1994. A Brownian dynamics study of direct ion passage through potassium channel. *Biologicheskie Membrany.* 11:209–216.

Villarroel, A., and B. Sakmann. 1992. Threonine in the selectivity filter of the acetylcholine receptor channel. *Biophys. J.* 62:196–208.

von Kitzing, E. 1995. Structure modeling of the acetylcholine receptor channel and related ligand gated channels. *In* Modelling of Biomolecular Structures and Mechanisms. A. Pullman, J. Jortner, and B. Pullman, editors. Kluwer Academic Publishers, Dortrecht. 39–57.

Vorobjev, Y. N., J. A. Grant, and H. A. Scheraga. 1992. A combined iterative and boundary element approach for solution of the nonlinear Poisson-Boltzmann equation. *J. Am. Chem. Soc.* 114:3189–3196.

Warshel, A. 1987. What about protein polarity? *Nature.* 330:15–16.

Weiner, S. J., P. A. Kollman, D. A. Case, U. C. Singh, C. Ghio, G. Alagona, S. J. Profeta, and P. Weiner. 1984. A new force field for molecular mechanical simulation of nucleic acids and proteins. *J. Am. Chem. Soc.* 106:765–784.

Zacharias, M., B. A. Luty, M. E. Davis, and J. A. McCammon. 1994. Combined conformational search and finite-difference Poisson-Boltzmann approach for flexible docking—application to an operator mutation in the lambda-repressor-operator complex. *J. Mol. Biol.* 238: 455–465.

Zauhar, R. J., and R. S. Morgan. 1985. A new method for computing the macromolecular electric potential. *J. Mol. Biol.* 186:815–820.

Zauhar, R. J., and R. S. Morgan. 1988. The rigorous computation of the molecular electric potential. *J. Comput. Chem.* 9:171–187.

Zhexin, X., H. Fuhua, and S. Yunyu. 1994. Calculation of solvation energy with a combination of the boundary element method and PDLD model. *J. Phys. Chem.* 98:12782–12788.